

Optimized Sampling of Mixed-State Observables

Marec W. Heger, Christiane P. Koch, and Daniel M. Reich*

¹*Theoretische Physik, Universität Kassel, Heinrich Plett-Straße 40, 34132 Kassel, Germany*

Quantum dynamical simulations of statistical ensembles pose a significant computational challenge due to the fact that mixed states need to be represented by a density matrix instead of a wave function. If the underlying dynamics is fully unitary, for example in coherent control at finite temperatures, one approach to approximate time-dependent observables in this context is to sample the density matrix by solving the Schrödinger equation for a set of wave functions with randomized phases. We show that, on average, random-phase wave functions perform well for ensembles with high mixedness, whereas at higher purities a deterministic sampling of the energetically lowest-lying eigenstates becomes superior. We find that the performance crossing point between these two approaches does not significantly depend on system dimension or desired error tolerance and is determined primarily through the ensemble purity. Moreover, we prove that minimization of the worst-case error for computing arbitrary observables is uniquely attained by eigenstate-based sampling. Finally, we point out how the structure of low-rank observables can be exploited to further improve eigenstate-based sampling schemes.

I. INTRODUCTION

In many molecular and condensed matter systems the efficient time propagation of statistical ensembles is crucial to properly model quantum dynamics under realistic conditions. Such incoherent states are most commonly described by density matrices which incorporate the concept of classical mixtures on top of quantum coherences [1]. However, the numerical treatment of density matrices proves to be challenging due to the requirement to store $\mathcal{O}(N^2)$ complex numbers for a general representation, where N is the underlying Hilbert space's dimension. Conversely, pure states in Hilbert space only requires the storage of at most $\mathcal{O}(N)$ complex entries. This issue is further exacerbated by the fact that, on top of the increased memory requirements, the computational effort is substantially larger, too. In the most general case, time propagation via solving the Schrödinger equation for pure states scales as $\mathcal{O}(N^2)$ which grows to $\mathcal{O}(N^4)$ when solving, e.g., the Liouville equation for density matrices.

A promising approach to reduce computational complexity is to find an effective description in Hilbert space. Methods to treat dissipative systems on the level of coherent states include, for example, Monte Carlo wave function techniques [2, 3], Keldysh contour methods [4], and the so-called Surrogate Hamiltonian [5, 6]. An interesting subclass of problems is given by mixed states which undergo coherent evolution. If no dissipative processes are present on the timescale of the dynamics, solving the Schrödinger equation of a complete set of Hilbert space states yields an exact representation of the system's time evolution, reducing the computational complexity from $\mathcal{O}(N^4)$ to $\mathcal{O}(N^3)$ [7]. This raises the question whether a further reduction could be achieved by preselecting an incomplete set of Hilbert space states.

The search for approaches in which one only considers a small subset of the total Hilbert space is motivated by the so-called eigenstate thermalization hypothesis [8–10]. It states that, under certain conditions, the behavior of the complete statistical ensemble is reproduced by individual energy eigenstates. As such one can expect that ensemble observables can already be approximated by considering only a small set of initial wave functions. A popular idea in this direction is the use of so-called random-phase thermal wave functions [11]. This method rests on the observation that while individual Hilbert space states can properly represent populations of an incoherent state they usually contain excess coherences. However, by randomizing the phases of these coherences using a set of random-phase thermal wave functions the superfluous contributions can be averaged out, thus restoring a proper description of the initial ensemble.

Such a stochastic approach has already been proven to yield well-converged results with a comparatively small number of random-phase realizations in applications such as photoassociation of Mg_2 dimers [12–14] and laser-induced rotation of SO_2 molecules [15]. However, its asymptotic behavior is rather poor, showing the well-known statistical $\sim \frac{1}{\sqrt{K}}$ tail where K is the number of realizations employed. Moreover, in contrast to using an orthonormal basis of the Hilbert space, the initial ensemble is not reobtained when K is equal to the Hilbert space dimension. This poses the question whether an approach using an orthogonal set of wave functions is superior to random-phase thermal wave functions in computing time-dependent expectation values.

Here we provide a theorem which uniquely identifies the best set of Hilbert space states if one aims to limit the worst-case approximation error of arbitrary time-dependent observables in mixed ensembles. In addition to the worst-case estimate we furthermore analyze the average behavior of this state set for arbitrary observables and compare it to the random-phase approach. Finally we also present ideas on how to use prior information

* daniel.reich@uni-kassel.de

about the target observables to engineer specific state sets which are most suitable to approximating the corresponding mixed-state expectation values.

The paper is organized as follows. Section II introduces the concept of wave-function sampling to simulate time-dependent ensemble expectation values. Section III introduces an error measure for the performance of a given sampling scheme and presents our central theorem on how to minimize the worst-case estimation error for arbitrary observables. In Section IV we discuss how different sampling schemes behave on average, with a particular emphasis on the dependence on temperature and Hilbert space dimension. Section V explores in how far prior information can be used to further optimize the sampling procedure. Finally, Section VI concludes.

II. RANDOM-PHASE THERMAL WAVE FUNCTIONS

A. Eigenstate-based Sampling

We start by considering an initial state in thermal equilibrium, i.e., a canonical ensemble and generalize to arbitrary mixed states in the following. The corresponding density operator is given by

$$\hat{\rho}_\beta = \frac{e^{-\beta\hat{H}_0}}{Z}, \quad (1)$$

where $Z = \text{tr}\{e^{-\beta\hat{H}_0}\}$ is the partition function, $\hat{H}_0 \equiv \hat{H}(t=0)$ the system Hamiltonian at initial time and $\beta = 1/(k_B T)$ the inverse temperature. We denote the eigenbasis of \hat{H}_0 as $\{|E_n\rangle\}_{n=1,\dots,N}$ with eigenenergies $\{E_n\}_{n=1,\dots,N}$. This diagonalizes the density matrix,

$$\hat{\rho}_\beta = \frac{1}{Z} \sum_{n=1}^N e^{-\beta E_n} |E_n\rangle \langle E_n|, \quad (2)$$

with N the Hilbert space dimension. Assuming coherent system dynamics, time propagation is mediated by the unitary time evolution operator, $\hat{U}(t)$, generated by the time-dependent Hamiltonian $\hat{H}(t)$. As a consequence, expectation values of observables at a certain time, $\langle \hat{A} \rangle_\beta$, can be obtained via solving the Schrödinger equation (instead of the Liouville equation for the full density matrix). Specifically, one can write

$$\begin{aligned} \langle \hat{A} \rangle_\beta &= \text{tr}[\hat{A}\hat{U}(t)\hat{\rho}_\beta\hat{U}^\dagger(t)] = \text{tr}[\hat{U}^\dagger(t)\hat{A}\hat{U}(t)\hat{\rho}_\beta] \\ &= \frac{1}{Z} \sum_{n=1}^N \langle E_n | \hat{U}^\dagger(t)\hat{A}\hat{U}(t)e^{-\beta E_n} | E_n \rangle \\ &= \sum_{n=1}^N p_n \langle E_n | \hat{U}^\dagger(t)\hat{A}\hat{U}(t) | E_n \rangle \\ &\quad \underbrace{\hspace{10em}}_{\equiv |\psi_n(t)\rangle} \\ &= \sum_{n=1}^N p_n \langle \psi_n(t) | \hat{A} | \psi_n(t) \rangle, \end{aligned} \quad (3)$$

with $p_n \equiv \frac{1}{Z}e^{-\beta E_n}$. As a result, the expectation value of an arbitrary observable can be computed exactly by Hilbert space propagation of a complete orthonormal basis. However, for systems with large Hilbert space dimension, this quickly becomes infeasible. This phenomenon is called the curse of dimensionality [16] leading to exponential scaling for each additional degree of freedom. One approach to reduce the numerical effort is truncation of Eq. (3) once the weights p_n become sufficiently small [7]. This approach is sensible for very cold ensembles, where the weights quickly drop off for excited states due to the Boltzmann factor $e^{-\beta E_n}$. For moderately warm ensembles the distribution broadens and, to our knowledge, no feasible way to predict the incurred error in the observable for a given cutoff point has been derived.

B. Thermal wave function sampling

Instead of using a truncated orthonormal eigenbasis, Gelman and Kosloff proposed random-phase thermal wave functions to approximate $\hat{\rho}_\beta$ and thereby compute time-dependent observables $\langle \hat{A} \rangle_\beta$ [11]. In a first step, a set of K non-orthogonal states, $\{|\Phi_k\rangle\}_{k=1,\dots,K}$, is constructed from some orthonormal basis $\{|\phi_j\rangle\}_{j=1,\dots,N}$,

$$|\Phi_k(\vec{\theta}^k)\rangle = \frac{1}{\sqrt{N}} \sum_{j=1}^N e^{i\theta_j^k} |\phi_j\rangle. \quad (4)$$

Each $|\Phi_k\rangle$ uses randomly chosen phases $\theta_j^k \in [0, 2\pi[$. The dyadic product $|\Phi_k\rangle \langle \Phi_k|$ is called realization,

$$|\Phi_k\rangle \langle \Phi_k| = \frac{1}{N} \sum_{j,j'=1}^N e^{i(\theta_j^k - \theta_{j'}^k)} |\phi_j\rangle \langle \phi_{j'}|. \quad (5)$$

By averaging an infinite number of realizations a resolution of the identity, $\hat{1}$, is obtained,

$$\hat{1} = \lim_{K \rightarrow \infty} \left(\frac{N}{K} \sum_{k=1}^K |\Phi_k\rangle \langle \Phi_k| \right). \quad (6)$$

Using Eq. (6), $\hat{\rho}_\beta$ can be expressed in random-phase thermal wave functions,

$$\begin{aligned} \hat{\rho}_\beta &= \frac{1}{Z} e^{-(\beta/2)\hat{H}_0} \hat{1} e^{-(\beta/2)\hat{H}_0} \\ &= \lim_{K \rightarrow \infty} \frac{N}{ZK} \sum_{k=1}^K e^{-(\beta/2)\hat{H}_0} |\Phi_k\rangle \langle \Phi_k| e^{-(\beta/2)\hat{H}_0} \\ &= \lim_{K \rightarrow \infty} \frac{N}{K} \sum_{k=1}^K \left| \Phi_k \left(\frac{\beta}{2}, \vec{\theta}^k \right) \right\rangle \left\langle \Phi_k \left(\frac{\beta}{2}, \vec{\theta}^k \right) \right|, \end{aligned} \quad (7)$$

with unnormalized $\left| \Phi_k \left(\frac{\beta}{2}, \vec{\theta}^k \right) \right\rangle \equiv Z^{-1/2} e^{-(\beta/2)\hat{H}_0} |\Phi_k\rangle$. Similarly to Eq. (3), the expectation value of an observ-

able \hat{A} is then obtained as

$$\langle \hat{A} \rangle_\beta = \lim_{K \rightarrow \infty} \frac{N}{K} \sum_{k=1}^K \left\langle \Phi \left(\frac{\beta}{2}, \vec{\theta}^k \right) \left| \hat{U}^\dagger(t) \hat{A} \hat{U}(t) \right| \Phi \left(\frac{\beta}{2}, \vec{\theta}^k \right) \right\rangle \quad (8)$$

In practice, the limit in Eq. (8) cannot be evaluated and some finite value of K needs to be chosen. Evidently, if $K > N$, using an orthonormal basis and employing Eq. (3) while propagating the full set of N energy eigenstates is always preferable. For $K < N$ the random-phase sampling approach directly competes with truncated eigenstate sampling. In the following we show that sampling from eigenstates is the optimal approach to construct thermal wave functions, if no prior knowledge of the system dynamics is available and arbitrary observables shall be determined. We then compare this procedure to the random-phase approach in terms of its average behavior instead of the worst-case behavior in Sec. IV A. Before we begin, we first define an error measure to quantify how well a certain construction of a thermal wave function performs regarding the approximation of time-dependent expectation values.

III. OPTIMAL SAMPLING FOR ARBITRARY OBSERVABLES

A. Error measure

From this point onwards, $\hat{\rho}_{\text{True}}$ denotes the initial density operator as given by Eq. (2) and $\hat{\rho}_{\text{Approx}}$ refers to any kind of approximation of the density matrix, e.g., the truncated versions of Eq. (2) or Eq. (7). We define the error of approximated expectation values when using the approximated density matrix $\hat{\rho}_{\text{Approx}}$ as

$$\varepsilon = \left| \text{tr}(\hat{A} \hat{U}(t) \hat{\rho}_{\text{True}} \hat{U}^\dagger(t)) - \text{tr}(\hat{A} \hat{U}(t) \hat{\rho}_{\text{Approx}} \hat{U}^\dagger(t)) \right|, \quad (9)$$

In the following we are interested in finding an upper bound for this error. Since the error scales linearly with the norm of the observable \hat{A} , we consider only observables with a fixed Hilbert-Schmidt norm which we assume to be equal to one without loss of generality. In particular, the error of an arbitrary observable with unit Hilbert-Schmidt norm is bounded from above in the following way,

$$\begin{aligned} \varepsilon &\leq \max_{\|\hat{A}\|_{\text{HS}}=1} \left| \text{tr}(\hat{A} \hat{U}(t) \hat{\rho}_{\text{True}} \hat{U}^\dagger(t)) - \text{tr}(\hat{A} \hat{U}(t) \hat{\rho}_{\text{Approx}} \hat{U}^\dagger(t)) \right| \\ &= \max_{\|\hat{A}\|_{\text{HS}}=1} \left| \text{tr}(\hat{U}^\dagger(t) \hat{A} \hat{U}(t) \hat{\rho}_{\text{Error}}) \right|, \end{aligned} \quad (10)$$

where we have used the abbreviation

$$\hat{\rho}_{\text{Error}} = \hat{\rho}_{\text{True}} - \hat{\rho}_{\text{Approx}}. \quad (11)$$

For observables with arbitrary Hilbert-Schmidt norm, the error bound can simply be obtained by multiplication

with the norm's value due to the homogeneity of the expression in \hat{A} . Equation (10) can be reexpressed by evaluating the trace using the eigenbasis of $\hat{\rho}_{\text{Error}}$ which we denote by $\{|\xi_i\rangle\}_{i=1,\dots,N}$:

$$\begin{aligned} \varepsilon &\leq \max_{\|\hat{A}\|_{\text{HS}}=1} \left| \text{tr}(\hat{U}^\dagger(t) \hat{A} \hat{U}(t) \hat{\rho}_{\text{Error}}) \right| \\ &= \max_{\|\hat{A}\|_{\text{HS}}=1} \left| \sum_{i=1}^N \langle \xi_i | \hat{A}(t) \hat{\rho}_{\text{Error}} | \xi_i \rangle \right| \\ &= \max_{\|\hat{A}\|_{\text{HS}}=1} \left| \sum_{i=1}^N \langle \xi_i | \hat{A}(t) \sum_{j=1}^N |\xi_j\rangle \langle \xi_j | \hat{\rho}_{\text{Error}} | \xi_i \rangle \right| \\ &= \max_{\|\hat{A}\|_{\text{HS}}=1} \left| \sum_{i=1}^N a_{ii}(t) \lambda_i \right|, \end{aligned} \quad (12)$$

where $\hat{A}(t) = \hat{U}^\dagger(t) \hat{A} \hat{U}(t)$ and $a_{ii}(t) = \langle \xi_i | \hat{A}(t) | \xi_i \rangle$. Here we have used completeness, $\hat{1} = \sum_{j=1}^N |\xi_j\rangle \langle \xi_j|$, as well as the relation $\langle \xi_j | \hat{\rho}_{\text{Error}} | \xi_i \rangle = \lambda_i \delta_{ij}$, where λ_i are the eigenvalues of $\hat{\rho}_{\text{Error}}$. Note that, due to the unitary invariance of the Hilbert-Schmidt norm, the relation $\|\hat{A}\|_{\text{HS}} = \|\hat{A}(t)\|_{\text{HS}}$ holds for all times t . Then Eq. (12) can be interpreted as a scalar product involving the vectorized quantities $(\vec{a})_i = a_{ii}(t)$ and $(\vec{\lambda})_i = \lambda_i$. Thus, the Cauchy-Schwarz inequality is applicable and it follows that

$$\begin{aligned} \varepsilon &\leq \max_{|\vec{a}| \leq 1} \left| \sum_{i=1}^N a_{ii}(t) \lambda_i \right| = \max_{|\vec{a}| \leq 1} |\vec{a} \cdot \vec{\lambda}| \\ &\leq \max_{|\vec{a}| \leq 1} |\vec{a}| \cdot |\vec{\lambda}| = |\vec{\lambda}| \\ &= \|\hat{\rho}_{\text{Error}}\|_{\text{HS}}. \end{aligned} \quad (13)$$

We have replaced $\|\hat{A}\|_{\text{HS}} = 1$ by $|\vec{a}| \leq 1$ since $|\vec{a}| = \sqrt{\sum_i a_{ii}^2} \leq \sqrt{\sum_{i,j} a_{ij}^2} = \|\hat{A}\|_{\text{HS}}$. Note that if \hat{A} and $\hat{\rho}_{\text{Error}}$ are parallel, i.e., identical up to a scalar factor, the inequalities in Eq. (13) all become equalities. In conclusion, we obtain for the approximation error ε the upper bound

$$\varepsilon \leq \|\hat{\rho}_{\text{Error}}\|_{\text{HS}} = \sqrt{\sum_{i,j} [(\hat{\rho}_{\text{Error}})_{ij}]^2}, \quad (14)$$

which holds for arbitrary observables and arbitrary system dynamics.

B. Optimal basis

The error bound in Eq. (14) is valid for any sampling method for $\hat{\rho}_{\text{Approx}}$. This raises the question of the optimal sampling method. The following theorem yields the lowest attainable worst-case error bound for Eq. (14) as well as the corresponding sampling method which achieves this error:

Theorem 1 Let $\hat{\varrho} \in \mathbb{C}^{N \times N}$ be an arbitrary Hermitian $N \times N$ matrix. Then, for all $\hat{M} \in \mathbb{C}^{N \times N}$ with $\text{rank}(\hat{M}) \leq K$, the inequality $\|\hat{\varrho} - \hat{M}\|_{\text{HS}}^2 \geq \sum_{i=K+1}^N |\lambda_i|^2$ holds, where $\{\lambda_i\}_{i=K+1, \dots, N}$ is the set containing the $N - K$ smallest eigenvalues of $\hat{\varrho}$. Equality is obtained if and only if $\hat{M} = \hat{P}\hat{\varrho}\hat{P}$, where \hat{P} is a projector onto the eigenspace corresponding to the eigenvalue set $\{\lambda_i\}_{i=1, \dots, N-K}$.

Proof

$$\begin{aligned} \|\hat{\varrho} - \hat{M}\|_{\text{HS}}^2 &= \langle \hat{\varrho} - \hat{M}, \hat{\varrho} - \hat{M} \rangle_{\text{HS}} \\ &= \|\hat{\varrho}\|_{\text{HS}}^2 + \|\hat{M}\|_{\text{HS}}^2 - 2\text{Re}\langle \hat{\varrho}, \hat{M} \rangle_{\text{HS}}. \end{aligned} \quad (15)$$

Since \hat{M} has at most rank K there exists a rank K projector \hat{P} such that $\hat{M} = \hat{P}\hat{M}\hat{P}$. It follows that

$$\begin{aligned} \text{Re}\langle \hat{\varrho}, \hat{M} \rangle_{\text{HS}} &\leq \left| \langle \hat{\varrho}, \hat{M} \rangle_{\text{HS}} \right| = \left| \text{Tr} \left[\hat{\varrho} \hat{P} \hat{M} \hat{P} \right] \right| \\ &= \left| \text{Tr} \left[\hat{P} \hat{\varrho} \hat{P} \hat{M} \hat{P} \right] \right| = \left| \langle \hat{P} \hat{\varrho} \hat{P}, \hat{P} \hat{M} \hat{P} \rangle_{\text{HS}} \right| \\ &\leq \|\hat{P} \hat{\varrho} \hat{P}\|_{\text{HS}} \|\hat{P} \hat{M} \hat{P}\|_{\text{HS}}. \end{aligned} \quad (16)$$

Here, the projector property $\hat{P} = \hat{P}^2$, invariance under cyclic permutation of the trace, and the Cauchy-Schwarz inequality have been used. Minimizing Eq. (15) translates into maximizing Eq. (16), where the maximum, i.e. equality, is given only if $\hat{P} \hat{M} \hat{P} \parallel \hat{P} \hat{\varrho} \hat{P} \Leftrightarrow \hat{P} \hat{M} \hat{P} = \mu \hat{P} \hat{\varrho} \hat{P}$ with $\mu \in \mathbb{C}$. Inserting this relation into Eq. (16), we obtain $\text{Re}(\mu) = |\mu|$ which implies $\mu \in \mathbb{R}_0^+$. In the following we focus on determining \hat{P} such that $\mu \|\hat{P} \hat{\varrho} \hat{P}\|_{\text{HS}}^2$ is maximal. This is obtained by plugging in this parallelity condition into the final expression in Eq. (16).

Representing $\hat{\varrho}$ and \hat{P} in a basis $\{|i\rangle\}_{i=1, \dots, N}$ which diagonalizes \hat{P} , i.e.,

$$\hat{P} = \sum_{i=1}^K |i\rangle \langle i| \quad \text{and} \quad \hat{\varrho} = \sum_{i,j=1}^N \varrho_{ij} |i\rangle \langle j|, \quad (17)$$

it follows that

$$\begin{aligned} \mu \|\hat{P} \hat{\varrho} \hat{P}\|_{\text{HS}}^2 &= \mu \text{Tr} \left[\hat{P} \hat{\varrho} \hat{P} \hat{P} \hat{\varrho} \hat{P} \right] \\ &= \mu \text{Tr} \left[\sum_{i,j,k=1}^K \varrho_{ij} \varrho_{jk} |i\rangle \langle k| \right] \\ &= \mu \sum_{i,j=1}^K \varrho_{ij} \varrho_{ji} = \mu \sum_{i,j=1}^K \varrho_{ij} \varrho_{ij}^* \\ &= \mu \sum_{i,j=1}^K |\varrho_{ij}|^2 = \mu \sum_{i,j=1}^K |\langle i| \hat{\varrho} |j\rangle|^2. \end{aligned}$$

Representing $\hat{\varrho}$ in its eigenbasis $\{|\phi_k\rangle\}_{k=1, \dots, N}$, i.e.,

$$\hat{\varrho} = \sum_{k=1}^N \lambda_k |\phi_k\rangle \langle \phi_k|, \quad (18)$$

with eigenvalues $\{\lambda_k\}_{k=1, \dots, N}$ sorted such that $\lambda_1 \geq \dots \geq \lambda_N$, Eq. (18) translates into

$$\begin{aligned} \mu \sum_{i,j=1}^K |\langle i| \hat{\varrho} |j\rangle|^2 &= \mu \sum_{i,j=1}^K \sum_{k=1}^N |\lambda_k|^2 |\langle i| \phi_k\rangle|^2 |\langle j| \phi_k\rangle|^2 \\ &= \mu \sum_{k=1}^N |\lambda_k|^2 \left[\sum_{i=1}^K |\langle i| \phi_k\rangle|^2 \right]^2. \end{aligned} \quad (19)$$

Now we define $z_k = \sum_{i=1}^K |\langle i| \phi_k\rangle|^2$. The inequality $z_k \leq 1$ holds since $\sum_{i=1}^K |\langle i| \phi_k\rangle|^2 \leq \sum_{i=1}^N |\langle i| \phi_k\rangle|^2 = 1$ applies. It directly follows that $z_k^2 \leq z_k \leq 1$ with $z_k^2 = z_k = 1$ if and only if $|\phi_k\rangle \in \text{im}(\hat{P})$, with $\text{im}(\hat{P})$ the image of \hat{P} . Furthermore $\sum_{k=1}^N z_k^2 \leq K$ holds with

$$\sum_{k=1}^N z_k^2 = K \Leftrightarrow \forall k: |\phi_k\rangle \in \text{im}(\hat{P}), \quad (20)$$

which can be seen as follows,

$$\begin{aligned} \sum_{k=1}^N z_k^2 &\leq \sum_{k=1}^N z_k = \sum_{k=1}^N \sum_{i=1}^K \langle i| \phi_k\rangle \langle \phi_k| i\rangle \\ &= \sum_{i=1}^K \langle i| i\rangle = K. \end{aligned} \quad (21)$$

Equations (18) and (19) imply, that

$$\lambda \|\hat{P} \hat{\varrho} \hat{P}\|_{\text{HS}}^2 = \mu \sum_{k=1}^N |\lambda_k|^2 z_k^2 \leq \mu \sum_{k=1}^K |\lambda_k|^2, \quad (22)$$

with equality if $z_k = 1$ when k is an index belonging to a set containing the K largest eigenvalues of $\hat{\varrho}$ and $z_k = 0$ otherwise. Thus $\text{im}(\hat{P})$ needs to be spanned by a set of eigenvectors corresponding to such an eigenvalue set.

Now we can finally rewrite Eq. (15),

$$\begin{aligned} \|\hat{\varrho} - \hat{M}\|_{\text{HS}}^2 &= \|\hat{\varrho}\|_{\text{HS}}^2 + \|\hat{P} \hat{M} \hat{P}\|_{\text{HS}}^2 - 2\text{Re}\langle \hat{\varrho}, \hat{M} \rangle_{\text{HS}} \\ &= \|\hat{\varrho}\|_{\text{HS}}^2 + \mu^2 \|\hat{P} \hat{\varrho} \hat{P}\|_{\text{HS}}^2 - 2\text{Re}\langle \hat{\varrho}, \hat{M} \rangle_{\text{HS}} \\ &\geq \|\hat{\varrho}\|_{\text{HS}}^2 + \mu^2 \|\hat{P} \hat{\varrho} \hat{P}\|_{\text{HS}}^2 - 2\mu \|\hat{P} \hat{\varrho} \hat{P}\|_{\text{HS}}^2, \end{aligned} \quad (23)$$

where we have used Eq. (16) in the final line. Searching for the extremum of this expression with respect to μ ,

$$0 \stackrel{!}{=} \frac{\partial}{\partial \mu} \|\hat{\varrho} - \hat{M}\|_{\text{HS}}^2 = (2\mu - 2) \|\hat{P} \hat{\varrho} \hat{P}\|_{\text{HS}}^2, \quad (24)$$

we find that $\mu = 1$ uniquely minimizes Eq. (23). Consequently,

$$\|\hat{\varrho} - \hat{M}\|_{\text{HS}}^2 \geq \sum_{k=K+1}^N |\lambda_k|^2 \quad (25)$$

holds with equality if and only if $\hat{M} = \hat{P} \hat{\varrho} \hat{P}$. This concludes the proof. \square

Theorem 1 can be applied to sampling mixed states via a set of pure states in the following way: Choose $\hat{\rho} = \hat{\rho}_{\text{True}}$ and $\hat{M} = \hat{\rho}_{\text{Approx}}$. Then constructing the density matrix $\hat{\rho}_{\text{Approx}}$ in the eigenbasis of $\hat{\rho}_{\text{True}}$,

$$(\hat{\rho}_\beta)_{ij} = \begin{cases} \frac{1}{Z} e^{-\beta E_i} & \text{if } i = j \text{ and } i < K, \\ 0 & \text{otherwise,} \end{cases} \quad (26)$$

minimizes the worst case for the error ε , cf. Eq. (10), uniquely. The first K diagonal entries of $\hat{\rho}_{\text{Approx}}$ are the largest eigenvalues of $\hat{\rho}_{\text{True}}$, hence the worst-case error can be estimated via

$$\begin{aligned} \varepsilon &\leq \|\hat{\rho}_{\text{True}} - \hat{\rho}_{\text{Approx}}\|_{\text{HS}} = \sqrt{\sum_{i=K+1}^N |\lambda_i|^2} \\ &= \frac{1}{Z} \sqrt{\sum_{i=K+1}^N |e^{-\beta E_i}|^2} \equiv \varepsilon_{\text{bound}}(K). \end{aligned} \quad (27)$$

This error bound only depends on the eigenvalues λ_i of $\hat{\rho}_{\text{True}}$. It is particularly small if the initial density matrix possesses a narrow population distribution. For thermal systems, this is usually connected to low temperatures. Furthermore, the error bound is independent of the actual system dynamics. As a result, if no prior information is available and one aims to minimize the worst-case error for computing observables of an ensemble, propagating the eigenvectors of the initial density matrix corresponding to the largest eigenvalues is the uniquely optimal choice.

IV. APPLICATION TO A SPIN CHAIN

A. General Observables

Theorem 1 proves that all randomized sampling methods, including random-phase thermal wave functions, have an inferior worst-case error bound compared to deterministic sampling using the lowest-lying eigenstates. However, we cannot yet make a statement on whether employing the optimal sampling method for the worst case is advantageous in a typical setting, i.e., *on average*, since the average error might behave quite differently from the worst-case bound. In order to elucidate this point we compare random-phase sampling of thermal wave functions with eigenstate-based sampling using the averaged results of randomized simulations. Specifically, we compute randomly drawn observables by generating random Hermitian matrices after a random unitary time evolution obtained by randomly generated unitaries with respect to the Haar measure [17].

To additionally gain insight into the scaling of the average error with Hilbert space dimension in a typical physical setting, we study the average error for a one-dimensional thermal spin chain with nearest-neighbor coupling, see, e.g., Refs. [18–20]. Increasing the length of

the spin chain doubles the Hilbert space dimension, exemplifying the curse of dimensionality present in almost all quantum systems. The corresponding Hamiltonian reads

$$\hat{H}(t) = -J \sum_{j=1}^{n-1} \hat{\sigma}_j^x \hat{\sigma}_{j+1}^x - h_z \sum_{j=1}^n \hat{\sigma}_j^z + \epsilon(t) \sum_{j=1}^n \hat{\sigma}_j^x, \quad (28)$$

with J the coupling strength, n the number of spins, h_z the field strength of an external magnetic field in z -direction and $\epsilon(t)$ representing a time-dependent magnetic field in x -direction with a truncated Gaussian envelope such that $\epsilon(t=0) = 0$. The vector operator $\hat{\sigma}_j = (\hat{\sigma}_j^x, \hat{\sigma}_j^y, \hat{\sigma}_j^z)$ contains the Pauli matrices acting on spin j .

Note that although the Hamiltonian in Eq. (28) possesses an explicit time dependence we can perform the analysis of the average error without carrying out the actual propagation. This can be understood as follows: An arbitrary observable, \hat{A} , can be decomposed into $\hat{A} = \hat{V} \hat{D} \hat{V}^\dagger$ with \hat{V} unitary and \hat{D} diagonal. We choose \hat{A} randomly by drawing a random \hat{D} , corresponding to a random spectrum of the observable \hat{A} , and a Haar measure random \hat{U} , corresponding to a random eigenbasis of the observable \hat{A} . Rewriting Eq. (9) using Eq. (10) leads to

$$\begin{aligned} \varepsilon &= \left| \text{tr}(\hat{A} \hat{U}(t) \hat{\rho}_{\text{Error}} \hat{U}^\dagger(t)) \right| \\ &= \left| \text{tr}(\hat{U}^\dagger(t) \hat{V} \hat{D} \hat{V}^\dagger \hat{U}(t) \hat{\rho}_{\text{Error}}) \right|, \end{aligned} \quad (29)$$

where the random \hat{V} and arbitrary time propagation $\hat{U}(t)$ can be combined into a single random unitary due to the fact that unitary matrices form a group. As such it is sufficient to draw random observables to capture the effect of random system dynamics and the error can be evaluated effectively at initial time $t = 0$. Even if the range of available system dynamics by choosing different fields $\epsilon(t)$ in Eq. (28) does not yield the full dynamic Lie algebra $\text{SU}(N)$ [21], drawing random observables still remains sufficient to emulate the additional effect of arbitrary dynamics. This follows from the very property of the Haar measure to be the unique left- and right-invariant measure on the group of unitary matrices. If \hat{U} is uniformly distributed with respect to the Haar measure, then both $\hat{W} \hat{U}$ as well as $\hat{U} \hat{W}$ are uniformly distributed for any unitary \hat{W} [22].

In the following we fix an error tolerance according to Eq. (9) and then determine the number of states K as a fraction of the total Hilbert space dimension N , required to obtain an approximation within this tolerance. We call this quantity, $F = \frac{K}{N}$, the fraction of states. The fraction of states required to stay within a specified tolerance $\varepsilon_{\text{bound}}$ in Eq. (27) will be called $F_{\text{bound}}^{\text{eigen}}$. The fraction of states needed to approximate, on average, the true expectation value of a random observable within this tolerance will be called $F_{\text{true}}^{\text{eigen}}$ for eigenstate-based sampling and $F_{\text{true}}^{\text{random}}$ for the random-phase approach.

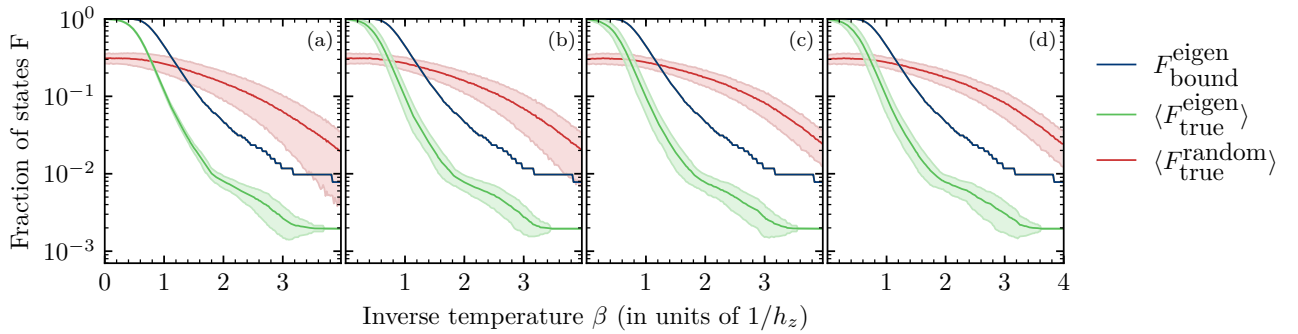


FIG. 1. Fraction of states required to obtain an error tolerance of $\varepsilon = 10^{-5}$ according to Theorem 1 (blue), when employing eigenstate-based sampling (green), or random-phase sampling (red). The Hilbert space dimension is $2^9 = 512$ and results from 128 random observables were averaged for the two sampling approaches. The four panels show results obtained for a set of observables with (a) rank 1, (b) rank 4, (c) rank 128, and (d) rank 512.

We first inspect the behavior of the required fraction of states for random observables with a given rank. This analysis offers a first glimpse into the question whether prior information can be employed to improve the sampling approach systematically. We will discuss this specific aspect in much greater detail in Sec. IV B. In particular, eigenstate-based sampling is working well provided the initial density matrix is effectively of low rank, i.e., the initial population distribution is narrowly peaked. This raises the question whether the performance of the different sampling schemes also depends on observable rank. The four panels of Fig. 1 compare the fraction of states as a function of inverse temperature for randomly generated observables with different rank, increasing from left (projector observables with rank 1) to right (full-rank observables with rank equal to the Hilbert space's dimension). The average fraction of states needed to stay within an error tolerance of 10^{-5} is displayed as a solid line with a single standard deviation being indicated by the surrounding shaded area. It is immediately evident from Fig. 1, that the average performance of the sampling approaches does not depend on observable rank. Even in terms of the standard deviation, only a slight difference is visible: When the observable rank increases, the variance increases for the eigenstate-based sampling whereas it decreases for the random-phase approach. We attribute this behavior to the fact that the eigenstate-based approach always employs the same set of Hilbert-space states for the sampling. This leads to a decrease in variance if the amount of randomness, i.e., the observable rank, is lowered. Conversely, the random-phase approach is inherently statistical and increasing the amount of randomness on top will reduce the variance leading to a general regression to the mean by the law of large numbers. However, independently upon observable rank, the standard deviation for the eigenstate-based approach will go to zero if the temperature is sufficiently low which is clearly visible in Fig. 1 for inverse temperatures greater than 3.6. Then, almost all of the population is gathered in the ground state and the vast majority of randomly generated observables only requires this single

state to reach the desired accuracy.

The fraction of states required for the eigenstate-based approach, $F_{\text{true}}^{\text{eigen}}$, always stays below the worst-case limit given by $F_{\text{bound}}^{\text{eigen}}$ in Fig. 1. This is in agreement with Theorem 1 which guarantees to stay below the given error threshold if one uses at least the corresponding number of states K given by Eq. (27). In contrast, the random-phase approach does not ensure such a behavior which can be seen for low temperatures in all four panels: The random-phase approach requires on average a much larger amount of states to stay below the error threshold. Conversely, the random-phase approach performs rather well at high temperatures where the eigenstate-based approach loses its advantage for larger β . In this regime a random state will be a better representative of the system's properties than the energetically lowest-lying states. This is because at high temperatures the eigenstate-based approach will never capture the behavior of the higher-lying states in the sampling process un-

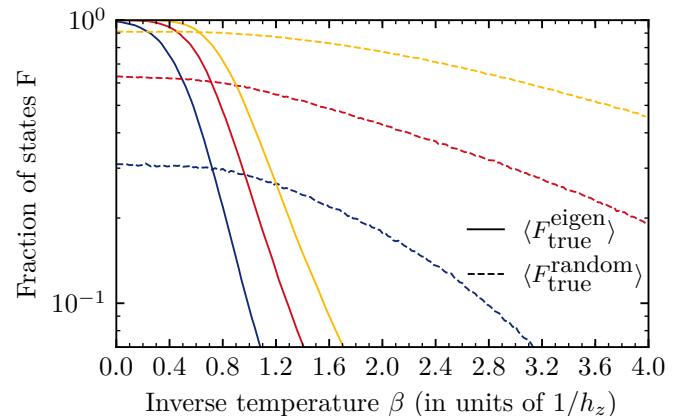


FIG. 2. Average fraction of states for eigenbasis sampling (solid lines) and for thermal wave function sampling (dashed lines) with $\varepsilon_{\text{bound}} = 10^{-5}$ (blue), $\varepsilon_{\text{bound}} = 10^{-6}$ (red), and $\varepsilon_{\text{bound}} = 10^{-7}$ (yellow). The Hilbert space dimension is $2^9 = 512$ and results from 128 random observables were averaged.

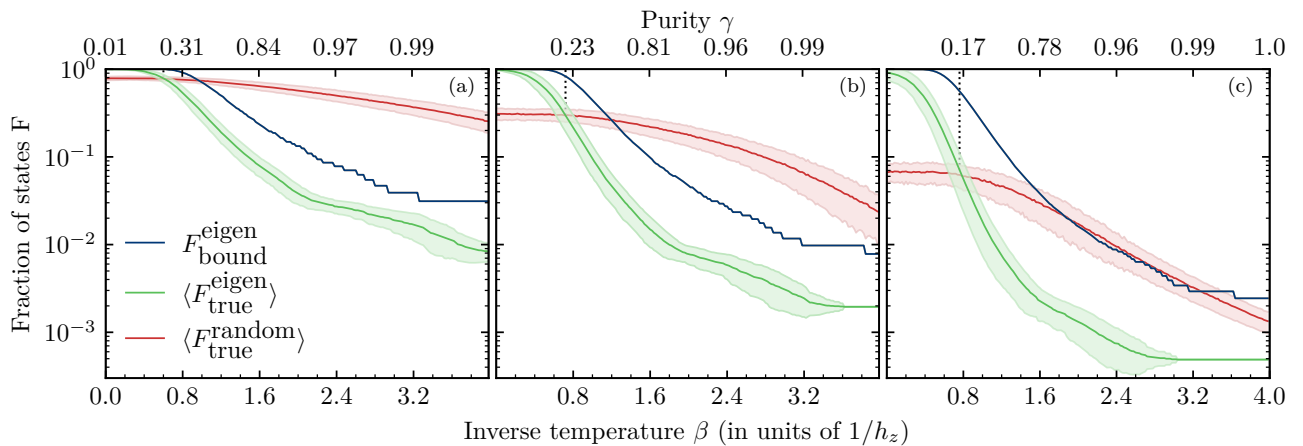


FIG. 3. Average fraction of states required for a set of 128 full-rank random observables for a spin chain with Hilbert space dimension (a) $2^7 = 128$, (b) $2^9 = 512$, and (c) $2^{11} = 2048$. The vertical dotted black line indicates the performance crossing point for random-phase and eigenstate-based sampling. ($\varepsilon_{\text{bound}} = 10^{-5}$)

til the sample size approaches the Hilbert space dimension. Such a flaw is absent in the random-phase approach which treats all eigenstates identically without imposing a hierarchy based on their populations. Essentially, it is the lack of this hierarchy, proving to be a fundamental disadvantage for low-temperature ensembles, which allows the random-phase approach to perform well at high temperatures. Note, however, that even for high temperatures the worst-case behavior for random-phase wave functions is still inferior to any deterministic approach according to Theorem 1. It is only the average performance which is superior.

Secondly, we analyze the scaling of the approximated expectation values with the desired error tolerances. Figure 2 shows the average fraction of states for eigenstate-based sampling and for random-phase sampling with respect to $\varepsilon_{\text{bound}} = 10^{-5}$, $\varepsilon_{\text{bound}} = 10^{-6}$ and $\varepsilon_{\text{bound}} = 10^{-7}$. Note that although $\varepsilon_{\text{bound}}$ is an absolute error, the normalization condition $\|\hat{A}\|_{\text{HS}} = 1$ for the random observables establishes an upper bound for the expectation value of 1. Therefore our choice of error tolerances between 10^{-5} and 10^{-7} can still be interpreted as a measure of relative precision.

From Fig. 2 one can immediately observe that the average fraction of states for eigenstate-based sampling shifts rather homogeneously with respect to temperature. In particular this implies that the increase in the required number of states is largely independent of ensemble purity. Such a behavior is also observed for the bounds given by Theorem 1 corresponding to the eigenstate-based sampling (data not shown). Conversely, random-phase wave functions appear to suffer more from a high accuracy requirement since not only does the graph for the required number of states shift upwards with decreased error tolerance but one can also observe a decrease in its slope and a sharp increase in its offset. Specifically, for medium and high temperatures a general increase of the required fraction of states is observed

in Fig. 2 when the error tolerance is lowered. At low temperatures the reduced slope further deteriorates the random-phase performance.

Next, we examine the performance of the sampling methods when the Hilbert space dimension increases. As mentioned above, once the Hilbert space becomes sufficiently large one might expect that the law of large numbers improves the performance of the random-phase approach due to its inherent stochasticity. The three panels of Fig. 3 compare the fraction of states required to stay within a tolerance of 10^{-5} for a system of 7 to 11 spins according to the bound from Theorem 1 and when using eigenstate-based and random-phase sampling. The position of the performance crossing points is indicated by a vertical dotted line. The behavior of the sampling approaches with increasing Hilbert space dimension is similar to the observed trend with reduced error tolerance in Fig. 2, but the curves move in the opposite direction. Notably, the required fraction of states for random-phase thermal wave function improves for all temperatures by a strong reduction in offset, with additional improvement for medium to low temperatures by an increase in slope. This confirms our conjecture that, for large Hilbert spaces, convergence is aided by the law of large numbers. In particular for high temperatures, i.e., low β , thermal wave functions become statistically more and more orthogonal when the dimensionality increases. This closes the gap to eigenstate-based sampling¹ and reinforces the suitability of the random-phase approach for large and thermally hot systems.

¹ In fact, if $T \rightarrow \infty$ then deterministically choosing the phases of thermal wave functions such that they are elements of a mutually unbiased basis [23] with respect to the energy eigenbasis is optimal. In this case the thermal wave functions form an orthogonal set while populations still remain perfectly described by any individual wave function. In particular, if $K = N$, an exact resolution of identity is reobtained.

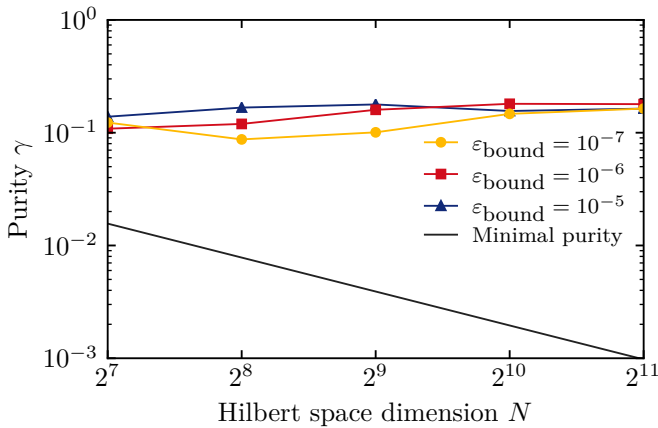


FIG. 4. Performance crossing points in terms of purity for random-phase and eigenstate-based sampling for spin chains with Hilbert space dimension between $2^7 = 128$ and $2^{11} = 2048$. For reference, the minimal possible purity $\frac{1}{N}$ in the corresponding Hilbert space is indicated.

Up to this point we have analyzed the behavior of the sampling approaches mainly with respect to the inverse temperature β of the initial ensemble. This is natural when a thermal ensemble is considered. However, Theorem 1 makes no statement about the specific nature of the object being sampled. Therefore, we now turn to a more general description by examining the required fraction of states as a function of the purity γ of the initial ensemble. Not only does this allow us to generalize our results to non-thermal systems, but it also yields a more direct measure of the initial population distribution which, in the thermal case, also depends on the Hamiltonian's spectrum.

Figure 4 shows the purity at the performance crossing points for increasing Hilbert space dimension and three different error tolerances. If the purity is smaller than this value, then the random-phase approach performs better on average, otherwise eigenstate-based sampling is superior. Note, that the purity at the crossing point always remains in the interval $[0.08, 0.20]$. This suggests that the superior sampling method can be estimated solely in terms of the ensemble purity - independently of error tolerance and Hilbert space dimension.

Our results for the random-phase approach qualitatively agree with the work by Kallush and Fleischer who investigated the performance of random-phase wave functions for describing orientation and alignment of a thermal ensemble of SO_2 molecules subject to a terahertz pulse [15]. For high temperatures, they reported the required number of random-phase thermal wave functions to be almost independent of temperature. This is in good agreement with our Fig. 3. In fact, we find a plateau at high temperatures, i.e. low β , independent of observable rank, system dimension, and error tolerance. In the low-temperature regime they found the efficiency of the random-phase approach to deteriorate, requiring an increasing amount of realizations to obtain accurate results.

Although we also observed efficiency of random-phase sampling to decline for lower temperatures, the absolute number of states required to maintain a given error tolerance still decreases. Furthermore they estimated the computational cost of an exact calculation, i.e., propagating a complete orthonormal set of wave functions, to become comparable to random-phase sampling at about 30 K, which corresponds to a purity of $1.5 \cdot 10^{-2}$. Compared to our results shown in Fig. 4, this estimate differs by about one order of magnitude. We attribute these differences to two significant deviations of the approach by Kallush and Fleischer compared to ours. First, they only employed a heuristic criterion for the error incurred in their simulations instead of a specific error measure, cf. our Eq. (9). Second, they considered two very specific observables, whereas we have analyzed the average performance over a set of random observables. As we have already illustrated above, particular observables can behave quite differently compared to the average. We will explore this fact in more detail in the following section and discuss which properties of observables are particularly suitable for random-phase sampling.

B. Specific Observables

The difference in behavior between average and worst-case error indicates that specific observables can behave quite differently from the average over randomly drawn observables. This becomes particularly evident in the Heisenberg picture where observables are time-dependent. Plugging Eq. (4) into Eq. (8) with $|\phi_j\rangle = |E_j\rangle$, i.e. considering random-phase wave function with respect to the energy eigenbasis, we obtain

$$\langle \hat{A} \rangle_\beta = \lim_{K \rightarrow \infty} \frac{1}{K} \sum_{k=1}^K \sum_{j, j'=1}^N \sqrt{p_j p_{j'}} e^{i(\theta_j^k - \theta_{j'}^k)} a_{j, j'}(t), \quad (30)$$

with $a_{j, j'}(t) = \langle E_{j'} | \hat{U}^\dagger(t) \hat{A} \hat{U}(t) | E_j \rangle$. Separating the diagonal part yields

$$\begin{aligned} \langle \hat{A} \rangle_\beta &= \lim_{K \rightarrow \infty} \frac{1}{K} \sum_{k=1}^K \sum_{\substack{j, j'=1 \\ j \neq j'}}^N \sqrt{p_j p_{j'}} e^{i(\theta_j^k - \theta_{j'}^k)} a_{j, j'}(t) \\ &+ \sum_{j=1}^N p_j a_{j, j}(t). \end{aligned} \quad (31)$$

Note that the second term does not depend on the random phases that were drawn and yields the exact result even if only one realization is employed. In other words, if the operator at final time in the Heisenberg picture is close to diagonal in the energy eigenbasis, then thermal wave functions have a significant head start since they only need to converge the comparatively small off-diagonal contributions, $a_{j, j'}(t)$, from the first summand in Eq. (31). Generally speaking, when the time-propagated observable is diagonal, or at least close to

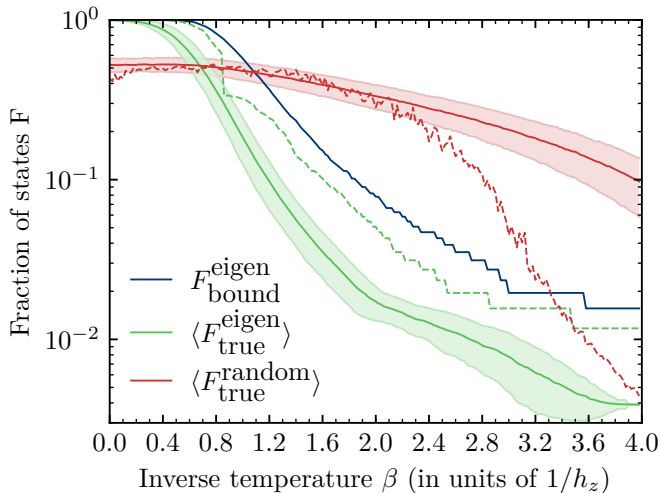


FIG. 5. Average fraction of states required for a set of 512 random observables for an 8-spin system ($N = 2^8 = 256$) with error tolerance $\epsilon_{\text{bound}} = 10^{-5}$ (solid lines, similar to Figs. 1 and 3). The required fraction of states for the \hat{A}_z operator with the same tolerance is indicated via dashed lines for eigenstate-based sampling (green) and the random-phase wave function approach (red).

diagonal, in the same basis as the initial ensemble, then random-phase wave functions as in Eq. (4) are particularly suitable.

As an example we consider the total polarization $\hat{A}_z = \sum_{j=1}^n \hat{\sigma}_j^z$ of the spin system described by the Hamiltonian in Eq. (28). At initial time this observable is diagonal with respect to the energy eigenbasis, since $[\hat{A}_z(t=0), \hat{H}(t=0)] = 0$. Our simulation parameters in atomic units are $h_z = 2$ and $J = \frac{1}{2}h_z$. The driving field $\epsilon(t)$ is given by a Gaussian pulse with a full-width at half maximum of $\frac{10}{h_z}$, an angular frequency of $\omega = \frac{5}{2}h_z$ and an amplitude of $\epsilon_0 = h_z$. While the perturbation introduced by this field destroys the diagonality of the total polarization in the Heisenberg picture, the observable at final time still remains close to diagonal if the field is weak. In the following, we compare the fraction of states for this specific Hamiltonian and observable to the average results obtained previously in Sec. IV A.

Figure 5 shows the average fraction of states for a system of 8 spins ($N = 256$) as solid lines with respect to deterministic sampling, statistical sampling and the corresponding bound by Theorem 1. The standard deviation is again marked by the shaded areas. This graph is similar to the one shown in Fig. 1. In addition the actual performance for both sampling methods in approximating the total polarization is displayed by dashed curves. Quite remarkably, the sampling approach via random-phase wave functions improves its performance by more than one order of magnitude below the standard deviation and even possesses a second performance crossing point compared to eigenstate-based

sampling (green dashed line) at around $\beta = 3.5$. Conversely, eigenstate-based sampling (red dashed line) performs rather poorly compared to the statistical average and lies above one standard deviation for almost all temperatures. Although this behavior agrees with our expectation, the effect is far more pronounced than anticipated. We attribute this to the fact that the diagonal matrix elements $\langle \psi_n(t) | \hat{A} | \psi_n(t) \rangle$ in Eq. (3) are ordered in such a way that the first eigenstates all underestimate the true expectation value while the latter eigenstates consistently overestimate it. Therefore a large number of eigenstates needs to be sampled to compensate for the initial underestimation. The statistical method under- and overestimates the true expectation value in each realization with the same probability and is thus immune to the ordering. While such structural effects can dominate the convergence behavior, their influence is typically hard to estimate, particularly if the propagation significantly alters the structure of the observable in the Heisenberg picture.

In conclusion, general observables are most efficiently sampled with the eigenstate-based approach if the initial density matrix has high purity whereas the random-phase approach becomes competitive at purities of around 0.1 – 0.2 and superior below this threshold. This behavior is mostly independent on observable rank and error tolerance. For specific observables this observation does not necessarily hold and individual features of the corresponding operators, in particular its diagonality in the initial ensemble’s eigenbasis, start to play an important role.

V. OPTIMAL SAMPLING FOR LOW RANK OBSERVABLES

For low-rank density matrices, such as thermal states at low temperatures, it is sufficient to propagate only few energy eigenstates, as evidenced by Eq. (3). For effectively high-rank density matrices, the required fraction of states for the eigenstate-based approach can become quite large, cf. Theorem 1. This behaviour is not influenced by particular features of the observable as it is exemplified by Fig. 1 which illustrates that sampling performance is almost completely independent on observable rank. However, the structure of the observable in relation to the initial density matrix does play a role, as evidenced by Sec. IV B. By swapping the role of observable and initial density matrix we are able to apply Theorem 1 to exploit structural effects on the level of the observable, specifically, we find an efficient sampling scheme for low-rank observables.

To this end we make use of the fact that the roles of initial density matrix and observable are interchangeable when calculating expectation values, due to cyclic invariance of the trace,

$$\text{tr}[\hat{A}\hat{U}(t)\hat{\rho}_\beta\hat{U}^\dagger(t)] = \text{tr}[\hat{U}^\dagger(t)\hat{A}\hat{U}(t)\hat{\rho}_\beta]. \quad (32)$$

Using this relation expectation values can be calculated via

$$\begin{aligned}
\langle \hat{A} \rangle_\beta(t) &= \text{tr}[\hat{U}^\dagger(t) \hat{A} \hat{U}(t) \hat{\rho}_\beta] \\
&= \sum_{n,m=1}^N \langle A_m | \hat{U}^\dagger(t) a_n | A_n \rangle \langle A_n | \hat{U}(t) \hat{\rho}_\beta | A_m \rangle \\
&= \sum_{n,m=1}^N a_n \langle A_n | \hat{U}(t) \hat{\rho}_\beta | A_m \rangle \langle A_m | \hat{U}^\dagger(t) | A_n \rangle \\
&= \sum_{n=1}^N a_n \langle A_n | \hat{U}(t) \hat{\rho}_\beta \underbrace{\hat{U}^\dagger(t) | A_n \rangle}_{|A_n(t)\rangle} \\
&= \sum_{n=1}^K a_n \langle A_n(t) | \hat{\rho}_\beta | A_n(t) \rangle, \tag{33}
\end{aligned}$$

where $\hat{A} = \sum_{n=1}^N a_n |A_n\rangle \langle A_n|$ with eigenvalues $\{a_n\}_{n=1,\dots,N}$ and eigenvectors $\{|A_n\rangle\}_{n=1,\dots,N}$. Note that $|A_n(t)\rangle = \hat{U}^\dagger(t) |A_n\rangle$ can be interpreted as a backwards-propagated eigenstate of the observable. The low rank of \hat{A} is important since any particular propagated eigenstate $|A_n(t)\rangle$ will not contribute to the sum in Eq. (33) if the corresponding eigenvalue a_n is zero. Since low rank operators possess a large number of vanishing eigenvalues only a small amount of states needs to be propagated. More generally, propagating the first K eigenstates corresponding to the K eigenvalues with the largest modulus leads to the following approximation of the observable \hat{A} (represented in its eigenbasis),

$$(\hat{A}_{\text{Approx}})_{ij} = \begin{cases} a_i & \text{if } i = j < K, \\ 0 & \text{otherwise,} \end{cases} \tag{34}$$

which, by Theorem 1, yields the smallest attainable worst-case error bound for arbitrary initial ensembles of

$$\varepsilon \leq \sqrt{\sum_{i=K+1}^N |a_i|^2}, \tag{35}$$

with ε being defined as in Eq. (9). In particular, if \hat{A} is of rank K and the corresponding K eigenstates are employed, then $\hat{A}_{\text{Approx}} = \hat{A}$ and therefore ε will vanish too. Note that the error bound still does not depend on the system dynamics. However, in contrast to sampling the initial density matrix, sampling the observable is independent upon any features of the ensemble, in particular its performance does not deteriorate for high temperatures / low purity.

An important example of low-rank observables is given by projectors. For example, simulations of thermal systems that require the measurement of populations in a set of bound states on specific electronic surfaces [13, 14] naturally give rise to such operators. The projector rank is equal to the number of bound states, which is typically much smaller than the total Hilbert space's dimension.

The only drawback of observable-based sampling is that the set of states that need to be propagated is tailored to the specific observable. Even though expectation values for arbitrary initial states can be approximated with the resulting set of propagated states, repeating the simulation for a different observable would require, in the worst case, the propagation of a completely different set of states. In short, sampling the observable is appropriate if one is interested in a single physical quantity for different initial states whereas sampling different observables for the same initial state is more suitably performed with the approach from Sec. III.

VI. CONCLUSIONS

We have shown that, with respect to minimizing the worst-case error, there is an optimal approach to compute arbitrary time-dependent observables in a statistical ensemble via pure-state sampling. It consists of using the lowest-lying energy eigenstates. The corresponding error is determined by the sum over the eigenvalues of the eigenstates that are not included in the sampling. The eigenstate-based sampling is the uniquely optimal choice. In particular, the worst-case sampling error is smaller than in any randomized sampling approach. Nevertheless the performance regarding the *average* error in a particular system for individual observables is only superior to random-phase sampling if the ensemble purity is relatively high or, in the language of thermal systems, the ensemble is cold. This can be attributed to the fact that eigenstate-based sampling is constructed hierarchically, starting from the energetically lowest-lying states. Thus, it might easily miss important contribution from high-lying states which start to play an important role once mixedness increases. For low purities a randomized approach provides on average a much more suitable coverage of Hilbert space.

Surprisingly, the threshold purity point where the average performance of random sampling surpasses the deterministic eigenstate-based approach seems to be almost independent of Hilbert space dimension. This is most likely due to the fact that the purity yields an absolute measure on the effective Hilbert space dimension since its value is dominated by the largest eigenvalues of the initial density matrix. Our results show that, on average, eigenstate-based approaches are superior above a purity of about 0.2 whereas below this value random-phase approaches perform better.

If one is only interested in particular physical quantities, then prior information about the structure of the corresponding observables can be exploited to refine the sampling scheme. Most notably, if the rank of the observable of interest is low, it is possible to propagate the eigenstates corresponding to the largest eigenvalues of the observables backwards in time. Then, one can compute the overlap of this backwards-propagated observable with the initial state at $t = 0$ to obtain the correspond-

ing expectation value. This works particularly well for low-dimensional projectors. For the special case of one-dimensional projectors, it implies propagation of a single wave function to be sufficient to compute the expectation values of arbitrary initial mixed state.

Although our notation and our examples were inspired by thermal states, we have made no assumptions on the particular physical nature of the initial state. Our main theorem and the methods of random-phase and eigenstate-based sampling can be employed for arbitrary statistical ensembles. The relevant eigenstates and eigenenergies in the general case are those of the initial density matrix instead of the Hamiltonian. We therefore expect our findings to be applicable not only to thermal states but also to different types of mixed states as encountered, for example, in mixed-state quantum computing [24, 25].

Our results on the possible methodological refinements employing prior information on system observables point towards the possibility to also exploit information on the system dynamics. For example, one could exploit the

fact that all mixed states possess no coherences in their eigenbasis. If the evolution does not introduce significant coherences and the observable is diagonal in this basis, then a single Hilbert space state is sufficient as long as it correctly reproduces the populations at $t = 0$. Saving numerical effort by adaptively focusing on only the most relevant part of Hilbert space is also at the core of many modern approaches in quantum chemistry, see, e.g., Refs. [26, 27], and condensed matter physics, see, e.g., Refs. [28, 29]. We expect that gaining more insight into the question of how to best perform such truncations will open up further avenues to fight the curse of dimensionality in quantum dynamics.

ACKNOWLEDGMENTS

Financial support by the Deutsche Forschungsgemeinschaft via the priority program SPP1840 QUTIF is gratefully acknowledged.

-
- [1] H. P. Breuer and F. Petruccione, *The Theory of Open Quantum Systems* (Oxford University Press, Great Clarendon Street, 2002).
 - [2] J. Dalibard, Y. Castin, and K. Mølmer, Phys. Rev. Lett. **68**, 580 (1992).
 - [3] C. W. Gardiner, A. S. Parkins, and P. Zoller, Phys. Rev. A **46**, 4363 (1992).
 - [4] L. M. Sieberer, M. Buchhold, and S. Diehl, Rep. Prog. Phys. **79**, 096001 (2016).
 - [5] C. P. Koch, T. Klüner, and R. Kosloff, J. Chem. Phys. **116**, 7983 (2002).
 - [6] C. P. Koch, T. Klüner, H. J. Freund, and R. Kosloff, Phys. Rev. Lett. **90**, 117601 (2003).
 - [7] C. P. Koch, R. Kosloff, E. Luc-Koenig, F. Masnou-Seeuws, and A. Crubellier, J. Phys. B: At., Mol. Opt. Phys. **39**, S1017 (2006).
 - [8] J. M. Deutsch, Phys. Rev. A **43**, 2046 (1991).
 - [9] M. Srednicki, Phys. Rev. E **50**, 888 (1994).
 - [10] M. Rigol, V. Dunjko, and M. Olshanii, Nature **452**, 854 (2008).
 - [11] D. Gelman and R. Kosloff, Chem. Phys. Lett. **381**, 129 (2003).
 - [12] L. Rybak, S. Amaran, L. Levin, M. Tomza, R. Moszynski, R. Kosloff, C. P. Koch, and Z. Amitay, Phys. Rev. Lett. **107**, 273001 (2011).
 - [13] S. Amaran, R. Kosloff, M. Tomza, W. Skomorowski, F. Pawowski, R. Moszynski, L. Rybak, L. Levin, Z. Amitay, J. M. Berglund, D. M. Reich, and C. P. Koch, J. Chem. Phys. **139**, 164124 (2013).
 - [14] L. Levin, W. Skomorowski, L. Rybak, R. Kosloff, C. P. Koch, and Z. Amitay, Phys. Rev. Lett. **114**, 233003 (2015).
 - [15] S. Kallush and S. Fleischer, Phys. Rev. A **91**, 063420 (2015).
 - [16] R. Bellman, *Dynamic Programming*, 1st ed. (Princeton University Press, Princeton, NJ, USA, 1957).
 - [17] F. Mezzadri, Notices Am. Math. Soc **54**, 592 (2007).
 - [18] G. K. Brennen and S. S. Bullock, Phys. Rev. A **70**, 052303 (2004).
 - [19] J. Maziero, H. Guzman, L. Céleri, M. Sarandy, and R. Serra, Phys. Rev. A **82**, 012106 (2010).
 - [20] M. A. Novotny, F. Jin, S. Yuan, S. Miyashita, H. De Raedt, and K. Michielsen, Phys. Rev. A **93**, 032110 (2016).
 - [21] D. d'Alessandro, *Introduction to quantum control and dynamics* (Chapman and Hall/CRC, 2007).
 - [22] M. Pozniak, K. Życzkowski, and M. Kus, J. Phys. A: Math. Gen. **31**, 1059 (1998).
 - [23] T. Durt, B.-G. Englert, I. Bengtsson, and K. Życzkowski, Int. J. Quantum Inf. **8**, 535 (2010).
 - [24] A. Ambainis, L. J. Schulman, and U. Vazirani, J. ACM **53**, 507 (2006).
 - [25] P. W. Shor and S. P. Jordan, Quantum Info. Comput. **8**, 681 (2008).
 - [26] J. B. Schriber and F. A. Evangelista, J. Chem. Phys. **144**, 161106 (2016).
 - [27] N. M. Tubman, J. Lee, T. Y. Takeshita, M. Head-Gordon, and K. B. Whaley, The Journal of chemical physics **145**, 044112 (2016).
 - [28] G. Gualdi and C. P. Koch, Physical Review A **88**, 022122 (2013).
 - [29] A. Go and A. J. Millis, Phys. Rev. B **96**, 085139 (2017).